JOURNAL OF Materials CHEMISTRY

Degradation mechanism of spinel $LiAl_{0.2}Mn_{1.8}O_4$ cathode materials on high temperature cycling

Y.-K. Sun,*[a] C. S. Yoon,[b] C. K. Kim,[b] S. G. Youn,[b] Y.-S. Lee,[c] M. Yoshio[c] and I.-H. Oh[d]

[a]*Department of Chemical Engineering, Hanyang University, Seoul 133-791, Korea. E-mail: yksun@hanyang.ac.kr*
[b]*Division of Materials Science and Engineering, Hanyang University, Seoul 133-791, Korea*
[c]*Department of Applied Chemistry, Saga University, Saga 840, Japan*
[d]*Division of Chemical Engineering, Korea Institute of Science and Technology, P.O. Box 131, CheongryangSeoul 130-650, Korea*

Received 25th April 2001, Accepted 20th June 2001
First published as an Advance Article on the web 16th August 2001

The structural degradation of the Al-doped spinel material, $LiAl_{0.2}Mn_{1.8}O_4$, before and after charge–discharge cycling in the 4 V region at elevated temperature has been studied by X-ray diffraction and high-resolution transmission electron microscopy. The capacity loss during cycling was noticeably increased with cell operation temperature from 50 to 80 °C. The formation of tetragonal $Li_2Mn_2O_4$ and the rocksalt phase Li_2MnO_3 in the spinel electrode cycled at elevated temperature could be responsible for the main cause of the capacity loss.

Introduction

Presently commercialized lithium-ion batteries use layer structured $LiCoO_2$ cathodes. Because of the high cost and toxicity of cobalt, an intensive search for new cathode materials has been investigated over the years. Spinel $LiMn_2O_4$ is one of the most promising cathode materials due to its low cost, abundance and non-toxicity.[1–5] However, while the spinel $LiMn_2O_4$ electrode shows good stability during cycling at room temperature, poor cycling behavior at elevated temperatures, *e.g.* 50–80 °C, is observed, which prevents its wider use as a cathode material for lithium secondary batteries.[6–8]

It is well known that the capacity loss for the $LiMn_2O_4$ electrode in the 4 V region at elevated temperatures is attributed to (1) a dissolution of the MnO into the electrolyte, and (2) a phase transition from cubic to tetragonal symmetry due to Jahn–Teller distortion.[9,10] Recently, Robertson *et al.* reported the presence of Li_2MnO_3 and spinel compositions other than $LiMn_2O_4$ in the cycled spinel electrode.[11] It was subsequently suggested by Cho and Thackeray that a capacity fade for the Li/$LiMn_2O_4$ cell cycled hundreds of times in the 4 V region at room temperature is due to the formation of Li_2MnO_3 at the particle surface resulting from dissolution of the MnO from $Li_2Mn_2O_4$.[12] However, there is not yet direct evidence for structural degradation for the spinel cycled electrode at elevated temperatures. In order to improve the cycleability of spinel $LiMn_2O_4$ electrodes at elevated temperatures, many research groups have studied cation substitution, anion substitution, and surface passivation treatment of $LiMn_2O_4$.[13–15] Although these attempts were effective to some extent for improving the cycling performance at 55 °C, the cycling behavior of the spinel $LiMn_2O_4$ at 80 °C was not reported.

The quality of $LiMn_2O_4$ powders used for lithium secondary batteries strongly depends on the synthetic method used. $LiMn_2O_4$ powders are typically prepared by a solid-state reaction which consists of extensive mechanical mixing and an extended grinding process which are detrimental to the quality of the final product. In order to obtain cathode materials with good homogeneity, uniform morphology and narrow particle-size distribution, a sol–gel method has been introduced. We have shown that phase-pure powdered spinels $Li_{1.03}Mn_2O_4$, $LiNi_{0.05}Mn_{1.95}O_4$ and $LiAl_{0.24}Mn_{1.76}O_{3.98}S_{0.02}$ with excellent rechargeability could be synthesized by the sol–gel method using various chelating agents.[16–18]

In this paper, we study the electrochemical cycling behavior and structural change of a $LiAl_{0.2}Mn_{1.8}O_4$ electrode after cycling in the 4 V region at elevated temperatures (50–80 °C) by means of X-ray diffraction (XRD) and high-resolution transmission electron microscopy (HRTEM). A structural degradation mechanism combined with capacity loss of the spinel $LiAl_{0.2}Mn_{1.8}O_4$ electrode at elevated temperature was investigated.

Experimental

$LiAl_{0.2}Mn_{1.8}O_4$ powders were prepared by a sol–gel method as reported in our previous work.[16,18] Powder X-ray diffraction (Rigaku, Rint-2000) using Cu-Kα radiation was used to identify the crystalline phase of cycled electrodes at various temperatures. The particle morphology of $LiAl_{0.2}Mn_{1.8}O_4$ powders was observed using a field emission scanning electron microscope (FE-SEM) (Hitachi Co., S-4100). Microstructures of individual oxide particles of the materials after cycling at various temperatures were also investigated by a transmission electron microscope (TEM, H-9000NA).

Charge–discharge cycles were performed in CR2030 button type cells. The cell consisted of a cathode and a lithium metal anode separated by a porous polypropylene film. For the fabrication of the electrode, the mixture, which contained 25 mg $LiAl_{0.2}Mn_{1.8}O_4$ powder and 15 mg conducting binder (10 mg Teflonized acetylene black (TAB) and 5 mg graphite), was pressed on a 2.0 cm^2 stainless screen at 800 kg cm^{-2}. The used electrolyte was a 1 : 2 (v/v) mixture of ethylene carbonate (EC) and dimethyl carbonate (DMC) containing 1 M $LiPF_6$. Charge–discharge cycles were performed galvanostatically at a current rate of C/3 (0.4 mA cm^{-2}) between 4.4 and 3.0 V.

Results and discussion

The as-prepared powders were confirmed to be well-defined spinel phases with space group *Fd3m* as shown in Fig. 1. The lattice constant (a) of the powders is 8.1814 Å which is lower than that of the stoichiometric spinel.[5] Generally, spinels with smaller lattice constants show improved cycleability. Recently,

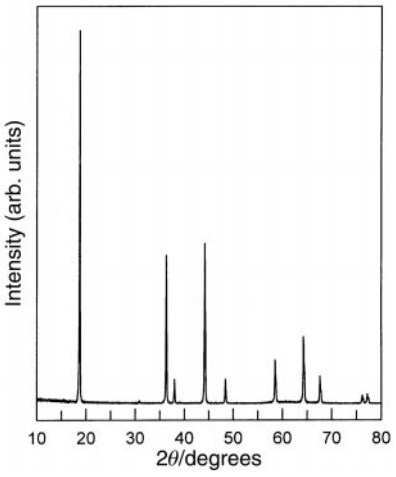

Fig. 1 X-Ray diffraction patterns for $LiAl_{0.2}Mn_{1.8}O_4$ powders.

Amatucci *et al.* reported that $LiAl_{0.2}Mn_{1.8}O_4$ synthesized by a solid-state technique had a lattice constant of 8.191(4) Å and showed a much improved cycleability at elevated temperature.[19] Previous reports revealed that the lattice constant of metal-doped $LiM_xMn_{2-x}O_4$ spinel structures decreases with increasing the amount of doped metal due to an increasing concentration of Mn^{4+} ions in the spinel structure by substituting Mn^{3+} ions with metal ions.[20]

Fig. 2 shows a scanning electron microscope (SEM) image for the as-prepared powders. The 2–10 μm particles show spherical and cubic gold crystal-like shapes and are quite different in morphology from the stoichiometric spinel which shows a well-developed (100) plane.

Fig. 3 shows the charge–discharge curves for the $LiAl_{0.2}Mn_{1.8}O_4$ electrode at 25, 50 and 80 °C with the corresponding discharge capacities as a function of cycle number shown in Fig. 4. The measured charge–discharge curves have only one plateau due to a large degree of Al substitution for Mn. While there were no differences between the charge–discharge curves for the $LiAl_{0.2}Mn_{1.8}O_4$ electrode at 25 and 50 °C, the polarization (voltage difference between the charge and discharge curves) of the electrode cycled at 80 °C increased with increasing cycle number. The electrode cycled at room temperature (25 °C) (Fig. 3(a)) delivers an initial capacity of 108 mA h g^{-1} and shows excellent cycling behavior retaining 99% (0.022 mA h g^{-1} $cycle^{-1}$) of the initial capacity after 50 cycles at the C/3 rate. Significantly, there is almost no capacity loss for the $LiAl_{0.2}Mn_{1.8}O_4$ electrode after 50 cycles at 50 °C (0.032 mA h g^{-1} $cycle^{-1}$), which is the lowest capacity loss observed so far at this temperature. The increased rechargeability of the $LiAl_{0.2}Mn_{1.8}O_4$ spinel electrode at 50 °C is attributed to a smaller lattice parameter and an excellent homogeneity of powders synthesized by the sol–gel method. The small lattice parameter (decrease of Mn^{3+} concentration) reduces the dissolution of the electrode surface and stabilizes

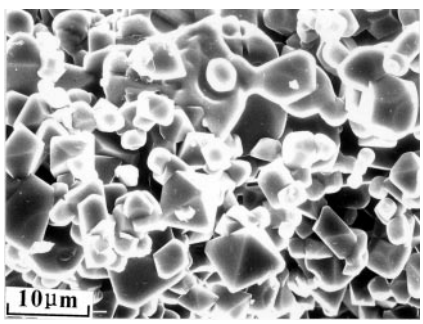

Fig. 2 Scanning electron micrograph of the $LiAl_{0.2}Mn_{1.8}O_4$ powders.

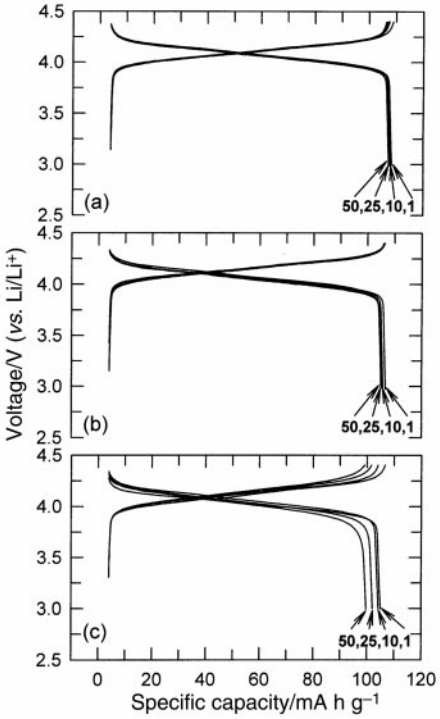

Fig. 3 Charge–discharge curves for $Li/LiAl_{0.2}Mn_{1.8}O_4$ cells at (a) 25, (b) 50 and (c) 80 °C as a function of cycle number.

the structural integrity of the active material as described in earlier reports.[19–21] In addition, the strength of the Al–O bond is another reason for the enhanced cycleability of the Al-doped $LiMn_2O_4$ electrode since this (512 kJ mol^{-1}) is stronger than that of Mn–O (402 kJ mol^{-1}).[22] This helps in reducing the structural disintegration of the material. On the other hand, the $Li/LiAl_{0.2}Mn_{1.8}O_4$ cell cycled at 80 °C initially delivers a discharge capacity of 105 mA h g^{-1} which decreases slowly during cycling to reach 99.7 mA h g^{-1} after 50 cycles with a capacity loss of 0.107 mA h g^{-1} $cycle^{-1}$. It should be noted that the capacity loss at 80 °C is much higher than that at 25 and 50 °C. The capacity loss during cycling is usually considered to be due to dissolution of Mn into the electrolyte solution.

XRD and high-resolution transmission electron micrograph (HRTEM) measurements were performed to investigate the degradation mechanism of the spinel $LiAl_{0.2}Mn_{1.8}O_4$ at elevated temperature. Fig. 5 shows the X-ray diffraction patterns for the $LiAl_{0.2}Mn_{1.8}O_4$ electrodes after 50 cycles at 25, 50 and 80 °C. For the cycled spinel electrodes at 25 and 50 °C, no structural changes were observed after 50 cycles; the

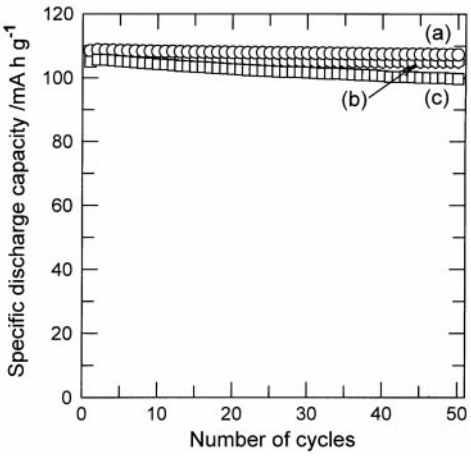

Fig. 4 Specific discharge capacity for the $Li/LiAl_{0.2}Mn_{1.8}O_4$ cell as a function of number of cycles at (a) 25, (b) 50 and (c) 80 °C.

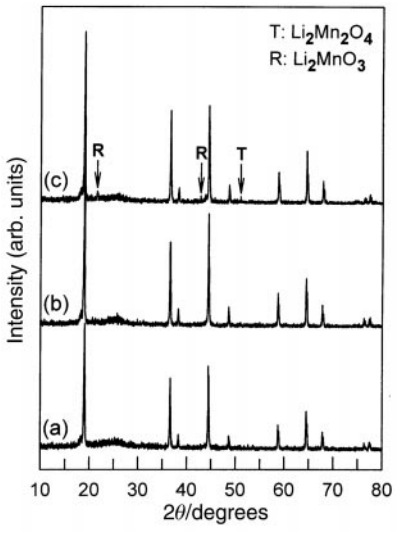

Fig. 5 X-Ray diffraction patterns for $LiAl_{0.2}Mn_{1.8}O_4$ electrodes after 50 cycles at (a) 25, (b) 50 and (c) 80 °C.

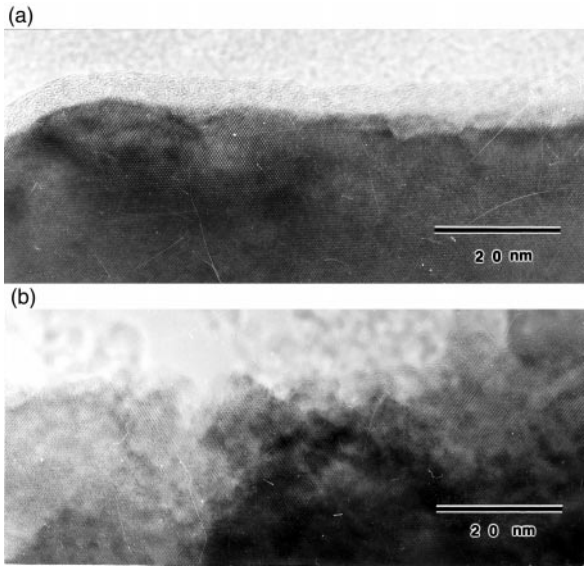

Fig. 7 HRTEM lattice image of the $LiAl_{0.2}Mn_{1.8}O_4$ electrodes after 50 cycles at (a) 25 and (b) 80 °C.

X-ray patterns of the cycled spinel materials (Fig. 5 (a) and (b)) were the same as those of the as-prepared powders (Fig. 1). However, for the cycled electrode at 80 °C, some low-intensty peaks were present that could be indexed to tetragonal $Li_2Mn_2O_4$ and rocksalt Li_2MnO_3 phases (Fig. 5(c)) though the characteristic peaks of the spinel phase were unchanged. The existence of those phases may be attributed to the capacity loss of the spinel electrode cycled at 80 °C. It was recently shown that tetragonal $Li_2Mn_2O_4$ occurs in discharged spinel electrodes cycled in the 4 V region at room temperature.[10,23]

To understand the phase transformation induced by the cycling at 80 °C in detail, TEM analysis was made with material previously used for the capacity cycle test, where the sample was analyzed in the fully discharged state (3 V). Fig. 6(a) shows a bright field micrograph of the powder after cycling at 25 °C. As can be seen, most particles still maintain the initial faceted morphology as observed in SEM even after 50 cycles and electron diffraction of the particle shown in the inset confirms that the particles still possessed a perfect spinel structure as indicated above by the XRD data. In contrast, the spinel electrode cycled at 80 °C appears to have lost its faceted morphology as seen in Fig. 6(b) where a rather irregular shape is evident. Furthermore, we have found structural differences within the particle as shown by the electron diffraction patterns. One region of the particle maintained the spinel structure as indicated by the {111} diffraction pattern (compare with Fig. 6 (a)) while the electron diffraction pattern taken in another part of the same particle showed extra spots superimposed on the {111} pattern. The lattice spacing corresponding to the extra spots did not belong to $LiMn_2O_4$, but closely matched those of the monoclinic Li_2MnO_3 phase ($C2/c$, $a=4.928$, $b=8.533$, $c=9.604$Å, $\beta=99.5°$, JCPDS[27-1252]). It appears that the electrolyte has preferentially attacked a localized part of the particle to convert the material to the Li_2MnO_3 phase at the surface through developing numerous stacking faults in the material.

Fig. 7(a) and (b) show HRTEM images of the {110} zone of the electrochemically cycled particles at 25 and 80 °C, respectively. The micrograph in Fig. 7(a) shows well-developed

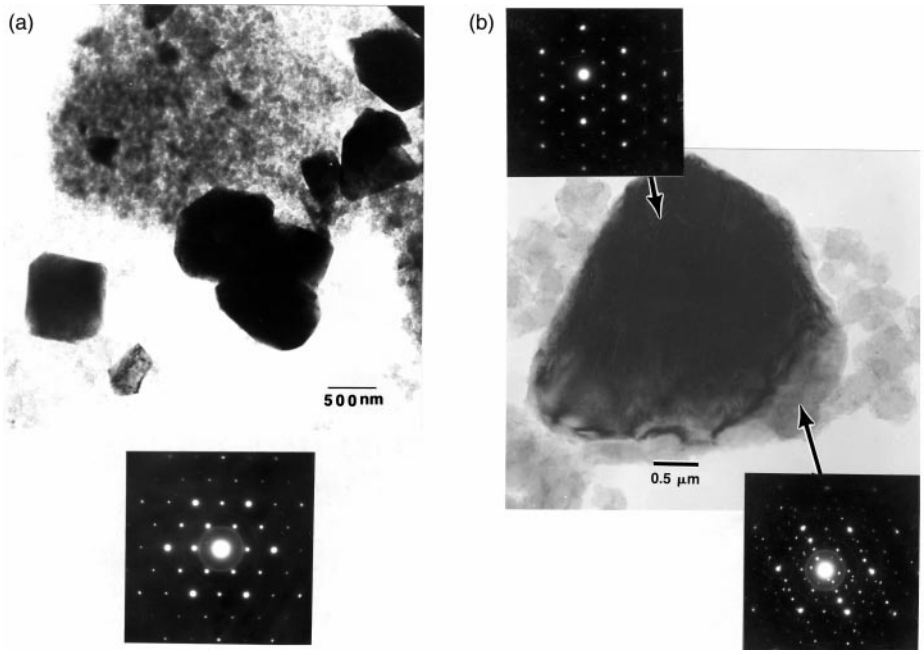

Fig. 6 Bright field images of the $LiAl_{0.2}Mn_{1.8}O_4$ electrodes cycled at different temperatures: (a) 25 °C with {111} zone electron diffraction, (b) 80 °C showing structural differences within the same particle.

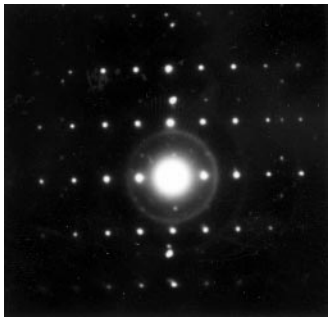

Fig. 8 Electron diffraction pattern of the tetragonal phase in the [111] zone found in the electrode after 50 cycles at 80 °C.

lattice fringes right to the particle edge with a comparatively uniform particle surface. In comparison, in the particle cycled at 80 °C (Fig. 7(b)), the smooth surface has been replaced by microscopically rough edges and the lattice fringes are not as well developed, which indicates that the particle surface has been substantially damaged by cycling in the electrode at elevated temperature. The Mn dissolution reaction, which is believed to be responsible for the capacity loss, appears to begin at the surface and progresses through the particles, developing structural faults in the process. Lastly, while searching for other relevant phases in the cycled electrode at 80 °C, we have found a particle possessing a symmetry (diffraction pattern shown in Fig. 8), that could only be indexed to $Li_2Mn_2O_4$ ($I4_1/amd$, $a=5.662$, $c=9.274$ Å, JCPDS[38-0294]) in the [111] zone with {101} peaks missing from the pattern. No such phase was evident in the powder cycled at 25 °C. Hence, TEM analysis confirms that although the tetragonal phase is not present to a substantial extent in the material cycled at 80 °C, its existence is related to the capacity loss at this temperature. The TEM results also agree well with the XRD data which show very weak peaks corresponding to $Li_2Mn_2O_4$ and support the XRD and HRTEM results that the existence of $Li_2Mn_2O_4$ and Li_2MnO_3 is responsible for the capacity loss at room and elevated temperatures.[12,24]

From the above results, the small capacity loss in the $Li/LiAl_{0.2}Mn_{1.8}O_4$ cell at elevated temperature is ascribed to a structural degradation of the spinel electrode and is associated with the formation of $Li_2Mn_2O_4$ and Li_2MnO_3. It is commonly accepted that dissolution of Mn as MnO plays an important role the capacity loss of spinel electrodes at elevated temperature. Although we could not directly observe the conversion process, from the XRD and TEM data it is concluded that the Li_2MnO_3 phase is created through the dissolution of MnO from $Li_2Mn_2O_4$ which is formed at the surface of the discharged $LiAl_{0.2}Mn_{1.8}O_4$ electrode due to kinetic limitations during the fast intercalation–deintercalation process ($Li_2Mn_2O_4 \rightarrow Li_2MnO_3 + MnO$).

Conclusions

An Al-doped spinel $LiAl_{0.2}Mn_{1.8}O_4$ electrode cycled at high temperature shows excellent cycleability at a high rate in the 4 V region. The capacity retention values of the electrode after 50 cycles at 25, 50 and 80 °C are 99, 98.5 and 95% of the initial capacity of 108, 107 and 105 mA h g^{-1}, respectively. This indicates that our prepared Al-doped spinel materials are good cathode materials which can compete with conventional cathode materials such as $LiCoO_2$ and $LiNi_{1-x}Co_xO_2$ for application in high temperature lithium batteries. Tetragonal $Li_2Mn_2O_4$ and rocksalt Li_2MnO_3 phases were detected at the surface of the discharged electrode after 50 cycles at 80 °C, which was the main cause of the capacity loss of the spinel electrode at this elevated temperature. The degradation mechanism of the spinel electrode is attributed to the formation of rocksalt Li_2MnO_3 that results from the dissolution of MnO from $Li_2Mn_2O_4$ into the electrolyte.

Acknowledgements

This work is supported in part by the Ministry of Information & Communication of Korea (“Support Project of University Information Technology Research Center” supervised by KIPA).

References

1 M. M. Thackeray, P. G. David, P. G. Bruce and J. B. Goodenough, *Mater. Res. Bull.*, 1983, **18**, 461.
2 T. Ohzuka, M. Kitagawa and T. Hirai, *J. Electrochem. Soc.*, 1990, **137**, 769.
3 D. Guyomard and J.-M. Tarascon, *Solid State Ionics*, 1994, **69**, 222.
4 R. J. Gummow, A. de Kock and M. M. Thackeray, *Solid State Ionics*, 1994, **69**, 59.
5 K. Amine, H. Tukamoto, H. Yasuda and Y. Fujita, *J. Electrochem. Soc.*, 1996, **143**, 1607.
6 G. G. Amatucci, C. N. Schmutz, A. Bylr, C. Siala, A. S. Gozdz, D. Larcher and J.-M. Tarascon, *J. Power Sources*, 1997, **69**, 11.
7 Y. Xia, Y. Zhou and M. Yoshio, *J. Electrochem. Soc.*, 1997, **144**, 2593.
8 H. Huang, C. A. Vincent and P. G. Bruce, *J. Electrochem. Soc.*, 1999, **146**, 481.
9 A. D. Pasquier, A. Blyr, P. Courjal, D. Larcher, G. Amatucci, B. Gerand and J.-M. Tarascon, *J. Electrochem. Soc.*, 1999, **146**, 428.
10 M. M. Thackeray, S. Yang, A. J. Kahaian, K. D. Kepler, E. Skinner, J. T. Vaughey and S. A. Hackney, *Electrochem. Solid-State Lett.*, 1998, **1**, 7.
11 A. D. Robertson, S. H. Lu and W. F. Howard Jr., *J. Electrochem. Soc.*, 1997, **144**, 3505.
12 J. Cho and M. M. Thackeray, *J. Electrochem. Soc.*, 1999, **146**, 3577.
13 Y. Xia, N. Kumada and M. Yoshio, *J. Power Sources*, 2000, **90**, 135.
14 G. G. Amatucci, A. Bylr, C. Signable, P. Alfonse and J.-M. Tarascon, *Solid State Ionics*, 1997, **104**, 13.
15 G. G. Amatucci and J.-M. Tarascon, *US Pat.*, 1997, 5,674,645.
16 Y.-K. Sun, *Solid State Ionics*, 1997, **100**, 115.
17 Y.-K. Sun and S.-H. Jin, *J. Mater. Chem.*, 1998, **8**, 2399.
18 Y.-K. Sun, Y.-S. Jeon and H. J. Lee, *Electrochem. Solid-State Lett.*, 2000, **3**, 7.
19 G. G. Amatucci, N. Pereira, T. Zheng and J.-M. Tarascon, *J. Electrochem. Soc.*, 2001, **146**, A171.
20 D. Song, H. Ikuta, T. Uchida and M. Wakihara, *Solid State Ionics*, 1999, **117**, 151.
21 Y.-K. Sun, K.-H. Lee, S.-I. Moon and I.-H. Oh, *Solid State Ionics*, 1998, **112**, 239.
22 J. A. Dean, *Lange's Handbook of Chemistry*, McGraw-Hill Inc., New York, 4th edn., 1992, 4.12–4.38,
23 W. Liu, K. Kowal and G. C. Farrington, *J. Electrochem. Soc.*, 1996, **143**, 3590.
24 Y.-K. Sun, *Electrochem. Commun.*, 2001, **3**, 199.